Available online at www.sciencedirect.com
ScienceDirect
Nuclear Physics B Proceedings Supplement 00 (2012) 1–6
Nuclear Physics B Proceedings Supplement

Studies of beauty and charm quark production and decays with the CMS

Luca Perrozzi on behalf of the CMS collaboration

P.O. box E27510 c/o CERN, CH-1211 Genve 23, Switzerland

Abstract

We review the recent results of the CMS experiment in the field of b-quark production, B hadron spectroscopy and decays. The beauty quark production cross section measurements are performed both in inclusive and exclusive channels. In addition, we present the observation of a new Ξ_b baryon and searches for rare charmed hadron decays.

Keywords:

1. Introduction

Heavy-Flavor (HF) physics at the Large Hadron Collider (LHC) is a powerful probe of quantum chromodynamics (QCD) at very high energies, providing a critical test of next-to-leading-order (NLO) calculations. In addition, knowledge of the HF final state properties can be used to search for physics beyond the Standard Model.

The CMS Experiment at LHC has a rich HF physics program thanks to the excellent performance of the wide-coverage muon system and the tracking system consisting of silicon pixels and strips. The CMS muon system is interlayered in the return yoke of the 3.8 T solenoid and surrounds the tracking system and the calorimeters of CMS up to a pseudorapidity of $|\eta| = 2.4$. A detailed description of the CMS detector, as well as more details on its subsystems and their performance, can be found elsewhere [1, 2, 3].

In 2010 the CMS experiment has collected an integrated luminosity of 40 pb^{-1} at $\sqrt{s} = 7\,\text{TeV}$ [4] with peak instantaneous luminosity of $2 \times 10^{32}\ \text{cm}^2\text{s}^{-1}$. The 2011 data taking period was characterized by a steep increase of the LHC instantaneous luminosity, reaching $3.5 \times 10^{33}\ \text{cm}^2\text{s}^{-1}$ with up to fifteen reconstructed primary vertices towards the end of the run. The total integrated luminosity is about 5 fb^{-1} [5].

Thanks to the flexible CMS trigger system the online selection algorithms were adapted to the increasing luminosity in a prompt and intelligent manner, by making use of invariant mass, decay length, distance of closest approach, transverse momentum, and rapidity.

This article is structured as follows: in Section 2 we summarize the status of B hadron searches and production measurements; in Section 3 we present the measurements of inclusive b-quark measurements; in Section 4 we review the recent searches for rare D^0 decays to dimuons. Conclusions are given in Section 5.

2. B hadrons

2.1. Observation of a new Ξ_b baryon

A new baryon has been observed in the decay $\Xi_\text{b}^{*0} \to \Xi_\text{b}^-\pi^+$ [6]. The reconstruction of such decays involves the presence of three secondary vertices, with $\Xi_\text{b}^- \to \text{J}/\psi\,\Xi^-$, $\text{J}/\psi \to \mu^+\mu^-$, $\Xi^- \to \Lambda^0\pi^-$, and $\Lambda^0 \to \text{p}\pi^-$. The analysis is based on the whole data sample of pp collisions at $\sqrt{s} = 7$ TeV collected in 2011. The trigger requires two opposite-sign muons compatible with being the decay products of a J/ψ, either promptly produced or displaced from the primary vertex (PV).

The reconstruction of the $\Xi_\text{b}^- \to \text{J}/\psi\,\Xi^-$ candidates begins by identifying $\text{J}/\psi \to \mu^+\mu^-$ decays, built by combining pairs muons satisfying the trigger conditions. Candidate Λ^0 baryons are reconstructed in decays to a pion (π_Λ) and a proton (p) with opposite charges, where the higher momentum track is assumed to be the proton. Candidate Ξ^- baryons are reconstructed by combining a

Λ^0 candidate with a track (π_Ξ) of the same charge as the π_Λ. The Ξ^- is then combined with the J/ψ to form a Ξ_b^- candidate with a kinematic vertex fit. The Ξ_b^- signal selection criteria are chosen by an iterative algorithm that maximizes both the signal yield and the significance.

To search for Ξ_b^{*0} baryons, the Ξ_b^- candidates are combined with tracks, assumed to be pions, with a charge opposite to the π_Ξ charge (opposite-sign pairs) using the mass difference Q between the measured J/$\psi\,\Xi^-\pi^+$ invariant mass and the sum of the masses of the decay products, $Q = M(\mathrm{J}/\psi\Xi^-\pi^+) - M(\mathrm{J}/\psi\Xi^-) - M(\pi)$, where $M(\pi)$ is the charged-pion mass [7].

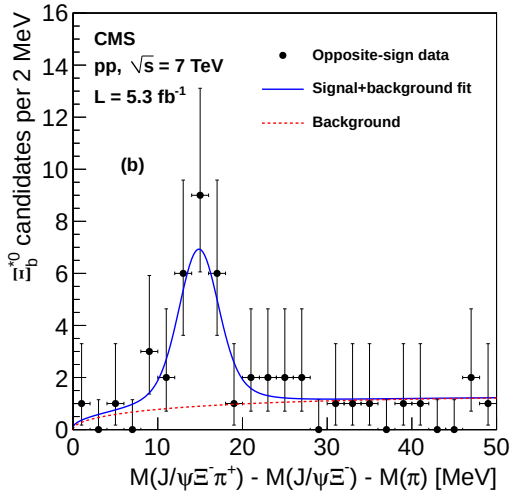

Figure 1: Q distribution in the $0 < Q < 50$ MeV range, along with the result of the signal-plus-background fit (blue solid curve); the background term is also shown (red dashed curve).

The measured Q distribution is displayed in Fig. 1 showing a clear excess in the region $12 < Q < 18$ MeV. An unbinned maximum-likelihood fit is performed to the opposite-sign Q distribution with a Breit–Wigner distribution convolved with a Gaussian function, added to the background function. The fitted parameters of the peak are $Q = 14.84 \pm 0.74$ (stat.) MeV and Breit–Wigner width $\Gamma = 2.1 \pm 1.7$ (stat.) MeV.

To evaluate the significance of the signal, the likelihood L_{s+b} of the signal-plus-background fit is determined. The fit is then repeated using the background-only model to obtain a new likelihood L_b. The logarithmic likelihood ratio $\sqrt{\ln(L_{s+b}/L_b)}$ results in a statistical significance of 6.9 standard deviations (σ). The background fluctuation probability, including the "look-elsewhere effect" in the range $0 < Q < 400$ MeV, has a significance of 5.3σ.

The systematic uncertainty on the measured Q value is evaluated with a detailed MC simulation. Two other sources of systematic uncertainties have been considered: the likelihood fit method and the choice of the selection requirements applied to the p_T of the tracks used for the measurement.

Given the charged-pion and Ξ_b^- masses [7], the resulting b-baryon mass is 5945.0 ± 0.7 (stat.) $\pm$ 0.3 (syst.) $\pm$ 2.7 (PDG) MeV. While the width of the new baryon is not measured with good statistical precision, it is compatible with theoretical expectations [8]. Given its measured mass and decay mode, the new baryon is likely to be the Ξ_b^{*0}, with $J^P = 3/2^+$.

The observation of this resonance, corresponding to the one observed in the charm sector [9], and its mass measurement add valuable information to the understanding of the interactions between quarks within a baryon.

2.2. *Observation of B_c^+ decays to $J/\Psi\pi$ and $J/\Psi\pi\pi\pi$*

The B_c^+ meson is the ground state of the bound $\bar{b}c$ system. It carries two different HF, complementing the studies performed with $c\bar{c}$ and $b\bar{b}$-quarkonia. The production mechanism for the $\bar{b}c$ meson differs in an essential way from that of a $b\bar{b}$ state, since two heavy quark-antiquark pairs must be created in a collision. In the B_c^+ weak decays, both c and b quark decays compete: the b quark decays with the c quark as a spectator or the c quark decays with b as a spectator.

The experimental studies of branching ratios and form factors would help understanding the hadronic matrix elements affected by non-perturbative physics. The first observation of approximately 20 B_c^+ events has been performed by the CDF Collaboration [10] in the semileptonic decay channel $B_c^+ \to J/\psi\, l^+\nu$, followed by $B_c^+ \to J/\psi\, \pi^+$. At the LHC a third mode $B_c^+ \to J/\psi\, \pi^+\pi^+\pi^-$ has been recently observed [11].

The CMS analysis [12] is based on the whole 2011 data sample considering unprescaled triggers with a displaced J/psi decay vertex It starts with the selection of the J/ψ candidates. B_c^+ candidates are then formed by combining the dimuon with one or three charged tracks in the event, assuming that they are pions. The signal cut selection has been optimized as a compromise between the yield and $S/\sqrt{(S+B)}$, where S is the signal and B the background.

The corresponding $B_c^+ \to J/\psi\, \pi^+$ candidate mass distribution is shown in Fig. 2, fitted with a Gaussian for the signal and a second order polynomial function accounting for the background.

The measured mass is 6.272 ± 0.003 (stat.) GeV/c^2 and its width is 0.026 ± 0.004 (stat.) GeV/c^2. The $S/\sqrt{(S+B)}$ ratio is 10.5.

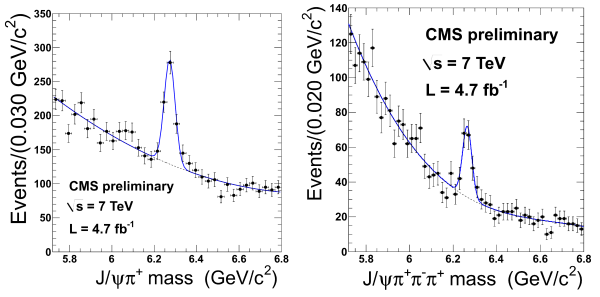

Figure 2: Left: $B_c^+ \to J/\psi\ \pi^+$ candidates invariant mass distribution. Right: $B_c^+ \to J/\psi\ \pi^+\pi^-\pi^+$ candidates invariant mass distribution.

The systematic uncertainty is accounted for by varying the fit function, the background model, the binning and the ranges of the fitted histograms. The $B_c^+ \to J/\psi\ \pi^+$ yield is 330 ± 36 (stat.) ±23 (syst.).

The $B_c^+ \to J/\psi\ \pi^+\pi^+\pi^-$ decay is the third and most recent experimentally observed mode. The first preliminary estimate of the ratio of branching ratios between decays with one and three pions has been presented by LHCb [11]. The search for this decay in CMS is performed by adding three charged hadrons to the J/ψ candidate in the event. Tighter selections are necessary to reduce the larger combinatorial background for the five-track compared to the three-track final-state.

The $J/\psi\ \pi^+\pi^+\pi^-$ signal, shown in Fig. 2, is fitted with a Gaussian for the signal and a third order polynomial function accounting for the background. The measured mass is 6.265 ± 0.004 (stat.) GeV/c^2 and its width is 0.021 ± 0.005 (stat.) GeV/c^2. The $S/\sqrt{S+B}$ ratio is 6.1 when evaluated in a mass range of ± 3 σ within the mass peak.

Systematic uncertainties include various histogram binnings, polynomial functions of different order for the background model, and different invariant-mass windows to perform the fit. The $B_c^+ \to J/\psi\ \pi^+\pi^+\pi^-$ yield is 108 ± 19 (stat.) ±14 (syst.).

2.3. *Measurement of the $\Lambda_b \to J/\Psi\Lambda$ cross section*

CMS reported the first measurement of the Λ_b baryon production cross section from fully reconstructed J/$\psi\,\Lambda$ decays in pp collisions at $\sqrt{s}$ = 7 TeV. This result complements the measurements of B^+ [13], B^0 [14], and B_s^0 [15] production cross sections also performed by CMS. The comparison of baryon production relative to meson production resulting from the same initial b-quark momentum spectrum allows for tests of differences in the hadronization process. Furthermore, the pp initial state at the LHC allows tests of baryon transport models [16, 17].

Events with Λ_b baryons reconstructed from their decays to the final state J/$\psi\,\Lambda$, with J/$\psi \to \mu^+\mu^-$ and $\Lambda \to p\pi$, are used to measure the differential cross sections $d\sigma/dp_T^{\Lambda_b} \times \mathcal{B}(\Lambda_b \to J/\psi\Lambda)$, $d\sigma/dy^{\Lambda_b} \times \mathcal{B}(\Lambda_b \to J/\psi\Lambda)$, and $\sigma(\overline{\Lambda}_b)/\sigma(\Lambda_b)$ with respect to the transverse momentum $p_T^{\Lambda_b}$ and the rapidity $|y^{\Lambda_b}|$, as well as the integrated cross section. The cross section times branching fraction measurements are averaged over particle and antiparticle states, while the ratio is computed by distinguishing the two states via decays to p or $\overline{p}$, respectively.

The data sample used in this analysis was collected by the CMS experiment in 2011 and corresponds to an integrated luminosity of 1.9 fb^{-1}.

Events are selected by requiring two oppositely charged muons. Displaced muon pairs from long-lived b-hadron decays are preferentially selected by further requiring a transverse separation from the mean pp collision position ("beamspot"). Opposite-sign muon pairs are fit to a common vertex to form J/ψ candidates, while Λ candidates are formed by fitting oppositely charged tracks to a common vertex. The Λ_b candidates are then formed by combining a J/ψ candidate with a Λ candidate with q vertex-constrained fit.

The efficiency for triggering on and reconstructing Λ_b baryons is computed with a combination of techniques using the data and large samples of fully simulated Monte Carlo (MC) signal events and is 0.73%.

To measure the ratio of antiparticle to particle cross sections $\sigma(\overline{\Lambda}_b)/\sigma(\Lambda_b)$, only the ratio of the Λ_b and $\overline{\Lambda}_b$ detection efficiencies is needed. Many of the efficiency contributions cancel in the ratio, including all the J/ψ and μ efficiencies since the particle and antiparticle states are indistinguishable. However, the Λ and $\overline{\Lambda}$ reconstruction efficiencies differ because of different interaction cross sections with the detector material.

The backgrounds are dominated by non prompt J/ψ from B hadron decays. The Λ_b proper decay length distribution in data confirms that the background events arise from long-lived b hadrons, and therefore offers no additional discriminating power between signal and background. The measured $m_{p\pi}$ distribution shows a purity of 77% genuine Λ events after applying the full selection criteria.

The Λ_b yields are extracted from unbinned extended maximum-likelihood fits to the $m_{J/\psi\,\Lambda}$ distribution in bins of $p_T^{\Lambda_b}$ and $|y^{\Lambda_b}|$. The ratio of antiparticle to particle yields is obtained by simultaneously fitting the Λ_b and $\overline{\Lambda}_b$ mass distributions, with resolution parameters fixed from the fit to the combined Λ_b and $\overline{\Lambda}_b$ simulated

sample and common mean allowed to float. The total number of signal events extracted from an inclusive fit is 1252 ± 42, where the uncertainty is statistical only.

The measured differential cross sections times branching fraction versus $p_{\mathrm{T}}^{\Lambda_{\mathrm{b}}}$ is shown in Fig. 3. compared to predictions from QCD calculations at LO and NLO accuracy. The measured p_{T} spectrum falls faster than predicted, while the $|y|$ spectrum shape is in agreement with the predictions within uncertainties.

The world-average b-quark fragmentation results assume that the fractions are the same for b jets originating from Z decays at LEP and directly from $\mathrm{p\bar{p}}$ collisions at the Tevatron. However, measurements of $f_{\Lambda_{\mathrm{b}}}$ performed at LEP [18, 19] and at the Tevatron [20] show discrepancies. A recent result [21] from the LHCb Collaboration measures a strong p_{T} dependence of the ratio of Λ_{b} production to B-meson production, $f_{\Lambda_{\mathrm{b}}}/(f_u + f_d)$, with $f_{\Lambda_{\mathrm{b}}} \equiv \mathcal{B}(b \to \Lambda_{\mathrm{b}})$ and $f_q \equiv \mathcal{B}(b \to \mathrm{B}_q)$. Larger $f_{\Lambda_{\mathrm{b}}}$ values are observed at lower p_{T}, which suggests that the discrepancy observed between the LEP and Tevatron data may be due to the lower p_{T} of the Λ_{b} baryons produced at the Tevatron.

A comparison of this and previous CMS results for b-hadron production versus p_{T} is shown in the bottom plot of Fig. 3, where the data are fit to the Tsallis function [22]. The fit indicates a more steeply falling p_{T} distribution than observed for the mesons, also suggesting that the production of Λ_{b} baryons, relative to B mesons, varies as a function of p_{T}, with a larger Λ_{b}/B ratio at lower transverse momentum.

The ratio $\sigma(\overline{\Lambda}_{\mathrm{b}})/\sigma(\Lambda_{\mathrm{b}})$ is found to be consistent with unity and constant as a function of both $p_{\mathrm{T}}^{\Lambda_{\mathrm{b}}}$ and $|y^{\Lambda_{\mathrm{b}}}|$, within the uncertainties, as predicted by MC. Therefore, no evidence of increased baryon production at forward pseudorapidities is observed within the available statistical precision for the kinematic regime investigated.

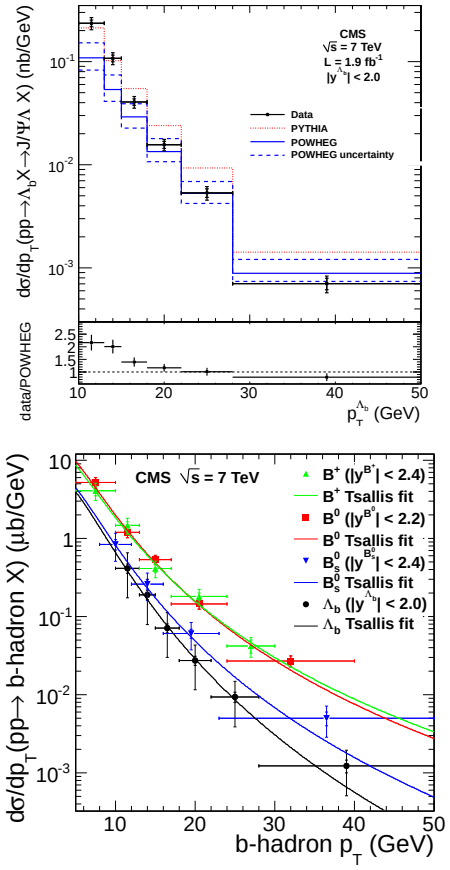

Figure 3: Top: measured differential cross sections times branching fraction $\mathrm{d}\sigma/\mathrm{d}p_{\mathrm{T}}^{\Lambda_{\mathrm{b}}} \times \mathcal{B}(\Lambda_{\mathrm{b}} \to \mathrm{J}/\psi\Lambda)$ compared to the theoretical predictions from PYTHIA and POWHEG. Bottom: comparison of production rates for B^+, B^0, $\mathrm{B}_{\mathrm{s}}^0$, and Λ_{b} versus p_{T}; fits to the Tsallis function for each distribution are also shown.

3. Inclusive *b* quark measurements

3.1. Measurement of the $bb \to \mu\mu$ cross section

The measurements of the cross section for the inclusive process $\mathrm{pp} \to \mathrm{b\bar{b}X} \to \mu\mu\mathrm{X}'$ allow for a comparison with QCD predictions in a kinematic domain where NLO calculations are more reliable because of the suppressed contribution of the gluon-splitting production mechanism (as discussed in [23] and the references therein).

In the CMS analysis [24] discrimination of the background is accomplished using the two-dimensional distribution of the two muon impact parameters (d_{xy}), defined as the distance of closest approach of each muon track to the interaction point projected onto the plane transverse to the beam axis.

The data employed for this measurement were collected during the 2010 running period corresponding to an integrated luminosity of 27.9 pb^{-1}. A sample of events with two muons, each with transverse momentum $p_{\mathrm{T}} > 3\,\mathrm{GeV}$ were selected at the trigger level. Further requirements, designed to increase the purity of the muon candidates and to increase the fraction of muons from b decay in the sample, are applied at the analysis stage.

Reconstructed muons in the simulated events are separated into four different classes, defined according to their origin: muons produced in the decay of a B hadron (B); muons from the semileptonic decays of charmed hadrons produced promptly (C); candidates originating from the primary vertex (P) muons produced in decays

of charged pions or kaons (P)

The single-particle distributions of the transverse impact parameter d_{xy} are obtained for each class from simulation and fit using analytical functions, from which the 2D templates are built symmetrically. The fractions of the individual contributions to the observed distribution are determined with a binned maximum-likelihood fit. Projections of the d_{xy} distributions with the results of the fits are shown in Fig. 4 for the two p_{T} selections.

In the data, the single-muon selection and trigger efficiencies are measured in intervals of p_{T} and η with the "tag-and-probe" method [2, 25].

The sources of systematic uncertainties are divided into uncertainties due to the model dependencies for both the signal and the backgrounds, the effects related to the impact parameter resolution, the fit method, and the measurement of the efficiency. They sum up to 8.9% (9.4%) for muon $p_{\mathrm{T}} > 4\,(6)$ GeV.

The measured cross sections are: $26.4 \pm 0.1\,(\mathrm{stat.}) \pm 2.4\,(\mathrm{syst.}) \pm 1.1\,(\mathrm{lumi.})$ nb and $5.12 \pm 0.03\,(\mathrm{stat.}) \pm 0.48\,(\mathrm{syst.}) \pm 0.20\,(\mathrm{lumi.})$ nb. for muon with $p_{\mathrm{T}} > 4$ GeV and $p_{\mathrm{T}} > 6$ GeV, respectively. The predicted cross sections with MC@NLO are: $19.7 \pm 0.3\,(\mathrm{stat.})\,^{+6.5}_{-4.1}\,(\mathrm{syst.})$ nb and $4.40 \pm 0.14\,(\mathrm{stat.})\,^{+1.10}_{-0.84}\,(\mathrm{syst.})$ nb. Both predictions are compatible with CMS measurements within the experimental and theoretical uncertainties

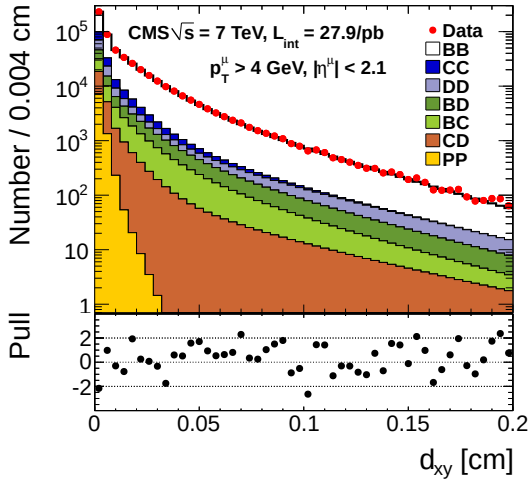

Figure 4: Top: Projected d_{xy} distributions from data with the results of the fit for muons with $p_{\mathrm{T}} > 4$ GeV. The distribution from each dimuon source is shown by the histograms. Bottom: The pull distribution from the fit.

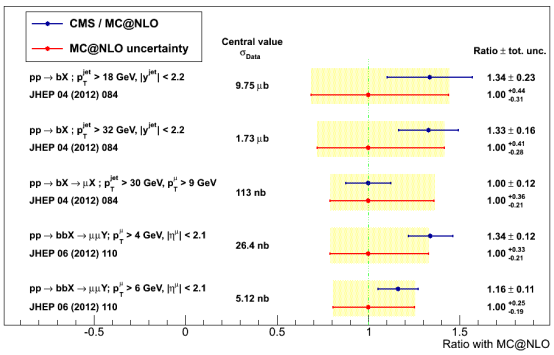

Figure 5: Ratio of measured and predicted b-quark cross sections.

3.2. *Summary of inclusive cross section measurements*

A summary of the inclusive cross sections measured in CMS, integrated over the measured pT and y ranges, and their ratios of with the NLO predictions are shown in Fig. 5. The measurements, probing b-quark production in different kinematic regions, are in agreement with the NLO QCD expectations although NLO predictions are often below the measurements. Theoretical uncertainties are always larger than the experimental ones.

4. Rare decays

In the SM, the flavour-changing neutral current (FCNC) decay $D^0 \to \mu^+\mu^-$ is highly suppressed, the branching ratio predicted by the standard model is about 10^{-13} [26]. However, other models can enhance these estimates by several orders of magnitude [27]. Since charm is an up-type quark, the search for FCNC in the charm sector is complementary to searches for FCNC decays of B and K mesons. The current best limit is set by the LHCb collaboration [28] to 1.3×10^{-8}(95% CL).

The CMS search for $D^0 \to \mu^+\mu^-$ [29] used a data sample corresponding to an integrated luminosity of 90 pb^{-1}, collected during 2010 and 2011. The strategy of the analysis is to measure the ratio of branching fractions, $(D^{*+} \to D^0\pi^+ \to \mu^-\mu^+\pi^+)/(D^{*+} \to D^0\pi^+ \to K^-\mu^+\nu\pi^+)$, so that most of the systematic uncertainties cancel out.

The $D^0 \to \mu^+\mu^-$ analysis requires two opposite-sign muon candidates, which must form a secondary vertex, which are combined with tracks which is given the pion mass to form a D^{*+} candidate. The reconstruction of the semileptonic decay mode, developed by E691 [30], is based on the decay chain $D^{*+} \to D^0\pi^+ \to K^-\mu^+\nu\pi^+$. In this case a kaon candidate is combined to an opposite-sign muon candidate to form a secondary vertex. Once

the direction between the primary and the secondary vertices is known, the E691 technique is used to determine the ν momentum. Due to the charge relation, each D^0 candidate can select a *right-sign* (RS) D^* candidate with $K^-\mu^+\pi^+$ and a *wrong-sign* (WS) D^* candidate with $K^-\mu^+\pi^-$. The WS sample is used to model the background of the RS sample.

Figure 6 shows the $\Delta M = M(K^-\mu^+\nu\pi^+) - M(K^-\mu^+\nu)$ distribution. The result of an unbinned fit is shown by the solid line in Figure 6. The fit returns $16\,458 \pm 204$ $D^0 \to K^-\mu^+\nu$ candidates.

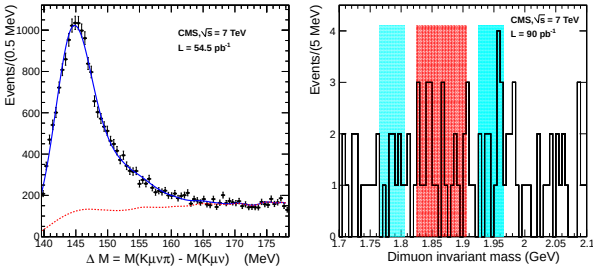

Figure 6: Left: distribution of $\Delta M = M(K^-\mu^+\nu\pi^+) - M(K^-\mu^+\nu)$ with the result of the fit superimposed. The points are the data, the blue solid line shows the fit result. The background function modeled from the WS distribution is shown as the dashed red line. Right: dimuon invariant-mass distribution in the $D^0 \to \mu^+\mu^-$ search region. The light-red band shows the signal region, while the two light-blue bands show the sideband regions

The $D^0 \to \mu^+\mu^-$ search region is defined as the $\mu^-\mu^+$ invariant-mass distribution obtained from the $\Delta M = M(\mu^+\mu^-\pi^+) - M(\mu^+\mu^-)$ distribution with the additional requirement $|\Delta M - \Delta M_{PDG}| < 3$ MeV, as shown in Fig. 6. No evidence for the $D^0 \to \mu^+\mu^-$ decay in the distribution is found.

The MC simulation is used to determine the acceptance and efficiency ratios for the signal and normalisation modes.

An exclusion limit on $N(\mu\mu)$ is determined by assuming that the number of events found in the signal region is the sum of signal and background events (both obeying Poisson statistics). The upper limit on the $D^0 \to \mu^+\mu^-$ branching fraction depends on the statistical and systematic uncertainties, the latter being dominated by the determination of the trigger efficiency. The exclusion limit at 90% CL is computed using the CL_s approach [31, 32]. The final result is: $\mathcal{B}(D^0 \to \mu^+\mu^-) \leq 5.4 \times 10^{-7}$(90% CL).

Although the present result is not the most stringent upper limit for this decay, it is the first analysis to use the semileptonic D^0 decay as normalisation mode.

5. Conclusions

In the past two years, the CMS experiment has carried out a a rich program of measurements in field of heavy flavour physics. Among the latest results, the first observation of a new baryon with beauty, the Ξ_b^{*0}, and the confirmation of two B_c^+ decay modes have been carried out. The $\Lambda_b \to J/\Psi\Lambda$ cross section has been measured and compared to the results previously obtained for the B mesons, finding differences in the p_T behavior which suggest a dependence of the b fragmentation on the transverse momentum. The inclusive cross sections for $b\bar{b}$ pair production into muons based on impact parameter have been measured and compared to QCD predictions. Lastly, a sarch for the rare decay $D^0 \to \mu^+\mu^-$ using for the first time the semileptonic D^0 as the normalisation mode has been performed.

References

[1] S. Chatrchyan, et al., JINST 3 (2008) S08004.
[2] CMS Collaboration, CMS Physics Analysis Summary CMS-PAS-MUO-10-002 (2010).
[3] CMS Collaboration, CMS Physics Analysis Summary CMS-PAS-TRK-10-005 (2010).
[4] CMS Collaboration, CMS Physics Analysis Summary CMS-PAS-EWK-10-004 (2010).
[5] CMS Collaboration, CMS Physics Analysis Summary CMS-PAS-SMP-12-008 (2012).
[6] S. Chatrchyan, et al., Phys. Rev. Lett. 108 (2012) 252002.
[7] K. Nakamura, et al., J. Phys. G 37 (2010) 075021.
[8] W. Detmold, C.-J. D. Lin, S. Meinel (2012). arXiv:1203.3378.
[9] P. Avery, et al., Phys. Rev. Lett. 75 (1995) 4364.
[10] F. Abe, et al., Phys. Rev. Lett. 81 (1998) 2432.
[11] LHCb Collaboration, submitted to *Phys. Rev. Lett.* (2012). arXiv:1204.0079v1.
[12] CMS Collaboration, CMS Physics Analysis Summary CMS-PAS-BPH-11-003 (2011).
[13] V. Khachatryan, et al., Phys. Rev. Lett. 106 (2011) 112001.
[14] S. Chatrchyan, Phys. Rev. Lett. 106 (2011) 252001.
[15] S. Chatrchyan, et al., Phys. Rev. D 84 (2011) 052008.
[16] G. Arakelyan, et al., Eur. Phys. J. C 54 (2008) 577.
[17] C. Merino, et al. (2011). arXiv:1105.6026.
[18] P. Abreu, et al., Z. Phys. C 68 (1995) 375.
[19] D. Buskulic, et al., Phys. Lett. B 384 (1996) 449.
[20] T. Aaltonen, et al., Phys. Rev. D 77 (2008) 072003.
[21] R. Aaij, et al., Phys. Rev. D 85 (2012) 032008.
[22] C. Tsallis, J. Stat. Phys. 52 (1988) 479.
[23] S. Frixione, M. L. Mangano, Nucl. Phys. B 483 (1997) 321.
[24] S. Chatrchyan, et al., JHEP 2012 (2012) 1–36.
[25] CMS Collaboration, CMS Physics Analysis Summary CMS-PAS-TRK-10-002 (2010).
[26] G. Burdnam, et al., Phys. Rev. D 66 (2002) 014009.
[27] E. Golowich, et al., Phys. Rev. D 79 (2009) 114030.
[28] LHCb Collaboration, Lhcb-conf-2012-005.
[29] CMS Collaboration, CMS Physics Analysis Summary CMS-PAS-BPH-11-017 (2012).
[30] E691 Collaboration, Phys. Rev. Lett. 62 (1989) 1587.
[31] A. Read, J. Phys. G 28 (2002) 2693.
[32] T. Junk, Nucl. Instr. Meth. A 434 (1999) 435.